

# Threshold generation of microwave harmonics in a solid-state plasma and parametric excitation of hypersound in bismuth

S. A. Vitkalov, V. F. Gantmakher, and G. I. Leviev

*Institute of Solid-State Physics, Academy of Sciences of the USSR, Chernogolovka, Moscow Province*  
(Submitted 10 November 1985)

Zh. Eksp. Teor. Fiz. **90**, 1493–1504 (April 1986)

A study is made of generation of microwave harmonics which form above a threshold intensity of a high-power electromagnetic wave incident on the surface of bismuth subjected to a strong magnetic field at liquid helium temperature. A theoretical model explaining this effect is constructed in the magnetohydrodynamic approximation. This model shows that an increase in the amplitude of an electromagnetic wave in bismuth creates an acoustic instability at the pump frequency and at multiples of this frequency. The threshold generation of harmonics is attributed to parametric excitation of hypersound. Experiments are reported in which a pump of  $0.91 \times 10^{10}$  Hz frequency was used to study the nature of the growth of the second harmonic power and the dependence of the threshold power of the incident wave on the temperature of a sample and the magnetic field applied to it. The experimental results are in agreement with the predictions of the theoretical model.

## 1. INTRODUCTION

The present authors discovered and investigated experimentally in detail<sup>1</sup> the phenomenon of threshold generation of harmonics of an electromagnetic wave of frequency  $\omega$  incident on the surface of bismuth subjected to a strong magnetic field  $H$ . When a certain threshold power of the incident wave  $P_{\omega}^{\text{th}}$  was reached, an instability appeared and resulted in growth of the second harmonic power  $P_{2\omega}$  in a characteristic time of the order of a few microseconds, and the difference between the powers  $P_{2\omega}$  at the beginning and end of a pulse reached 20–30 dB. The nature of the instability was not finally determined in Ref. 1, although it was pointed out there that at threshold powers the amplitude of the electric field  $E_{\omega}$  of a wave in the metal reached values at which the velocity of the transverse drift of carriers in the magnetic field  $v_{\omega} = c(E_{\omega}/H)$  became of the order of the velocity of sound  $s$ . Our aim will be to show that the threshold generation of the second harmonic is due to an acoustoelectronic instability associated with parametric generation of hypersound at frequencies  $\omega_s$  close to the frequency  $\omega$  or one of its multiples  $n\omega$ .

Studies of nonlinear effects due to a high drift velocity  $v$  of carriers in bismuth were started by Esaki.<sup>2</sup> He observed<sup>2</sup> a kink in the current-voltage characteristic of bismuth subjected to a transverse magnetic field  $H$ . This kink appeared in a field  $E$  in which this velocity became  $v = c(E/H) = s$ . The relationship between the Esaki effect and microwave nonlinear characteristics was discussed in Refs. 3 and 4.

The threshold behavior of a nonlinear response of bismuth was also reported in Refs. 3 and 5, but these experiments were carried out in weaker magnetic fields and the change in the nonlinear characteristics did not exceed 100%. It is not yet clear whether these effects are due to the same factors which are discussed below.

It was shown in Ref. 4 that if a sample carrying a constant current was subjected also to an electromagnetic wave,

the kink in the current-voltage characteristic was accompanied by a 20–30 dB increase in the power of the second harmonic  $P_{2\omega}$  of the electromagnetic wave. An analysis of the experimental results showed that the second harmonic is generated as a result of the following processes:

a) an electromagnetic wave incident on a sample generates sound at a frequency  $\omega_s = \omega$  near the surface;

b) the sound of frequency  $\omega_s$ , because of an acoustoelectronic instability induced by a constant current, is amplified and converted into higher harmonics, particularly into the second harmonic;

c) a hypersonic wave of frequency  $2\omega_s$  traveling near the surface is converted back into an electromagnetic wave.

The characteristic times of the transient processes observed in Ref. 4 in the course of generation of the second harmonic were of the order of  $1 \mu\text{sec}$ , i.e., they were the same as the corresponding times in the Esaki effect<sup>6</sup> and as in the threshold generation of harmonics,<sup>1</sup> and the enhancement of  $P_{2\omega}$  in Ref. 4 was close to that reported in Ref. 1. Essentially, the characteristics of the process of harmonic generation were similar in the presence of a constant drift velocity  $v$  (Ref. 4) and in its absence, but in the latter case the process occurred at a higher amplitude of  $E_{\omega}$  (Ref. 1) and this circumstance was the stimulus for the investigation reported below.

In the next section we shall present a theoretical model constructed in the magnetohydrodynamic approximation ignoring the quantum effects. We shall use this model to calculate the attenuation of sound under electromagnetic pumping conditions and show that when a certain threshold amplitude of the electromagnetic wave is exceeded the sign of the attenuation is reversed, i.e., hypersound is amplified. Some consequences of this model will be compared later with our experimental results. The relevant experiments are described in the third section. To supplement the experimental results in Ref. 1, we investigated the nature of the growth

of the harmonic power  $P_{2\omega}$  in time and the dependence of the threshold power  $P_{\omega}^{\text{th}}$  of the incident wave on the temperature of a sample and on the magnetic field  $H$  applied to it. In the last (fourth) section we shall compare the theory and experiment. This comparison shows quite convincingly that the threshold generation of higher harmonics<sup>1</sup> is due to an acoustoelectronic instability of hypersound which appears when bismuth is subjected to a strong electromagnetic wave of microwave frequency.

## 2. THEORETICAL MODEL

We shall write down a coupled system of equations for a magnetized electron-hole plasma and a neutral lattice. We shall describe the plasma in the hydrodynamic approximation and we shall allow for the interaction between the system of carriers and the lattice using the deformation potential:

$$m_{e,h} \left( \frac{\partial}{\partial t} + \mathbf{v}_{e,h} \nabla \right) \mathbf{v}_{e,h} = \mp e \left( \mathbf{E} + \frac{1}{c} [\mathbf{v}_{e,h} \mathbf{H}] \right) - Q_{e,h} \nabla^2 \mathbf{u} + \beta_{e,h} \nabla n_{e,h} - \frac{m_{e,h} \mathbf{v}_{e,h}}{\tau}, \quad (1)$$

$$\frac{\partial}{\partial t} n_{e,h} + \text{div} (n_{e,h} \mathbf{v}_{e,h}) = 0, \quad (2)$$

$$\text{div} \mathbf{j} = e \text{div} (n_h \mathbf{v}_h - n_e \mathbf{v}_e) = 0, \quad (3)$$

$$\partial^2 u / \partial t^2 - s^2 \nabla^2 u = \rho^{-1} (Q_e \nabla n_e + Q_h \nabla n_h). \quad (4)$$

Here,  $m_e$ ,  $v_e$ ,  $Q_e$ ,  $\beta_e$ , and  $n_e$  are the mass of electrons, their drift velocity, the deformation potential, a coefficient associated with electron diffusion, and the electron density, respectively; a similar notation is used for holes ( $h$ ). The other notation is as follows:  $s$  is the velocity of sound;  $\mathbf{u}$  is the lattice displacement;  $\tau$  is the relaxation time; the  $y$  axis along which the acoustic wave is propagating is perpendicular to the magnetic field  $\mathbf{H} \parallel z$ ; the carrier dispersion law is assumed to be isotropic; the electron-hole plasma is postulated to be completely compensated.

The validity of these equations is governed by the high intensity of the magnetic field: the cyclotron frequency  $\Omega$  is less than the plasma frequency, but higher than all the other characteristic frequencies,  $\Omega \gg \omega \gg 1/\tau$ , and the cyclotron radius  $R$  is less than all the other characteristic dimensions:  $qR \ll 1$  ( $q$  is the wave vector of sound). In fields of this kind the velocity of a magnetoplasma wave in bismuth is  $V \approx 10^9$  cm/sec, i.e.,  $V \gg s$ . We shall therefore ignore the wave vector  $\mathbf{k}$  of this wave and assume that the electric field of the wave is homogeneous in space.

For the sake of simplicity we shall henceforth assume that  $m_h \gg m_e$ . Then, the ambipolar diffusion coefficient is  $D = D_e = R_e^2 / 3\tau$ . Moreover, since the applied static magnetic field is high, we shall ignore the magnetic field of the wave in Eq. (1). The validity of this simplification can be demonstrated by retaining the term with an alternating magnetic field in the iteration process and comparing the values of the various nonlinear contributions: such a procedure shows that the nonlinearity is mainly due to the terms  $\nabla \mathbf{v} \nabla$  in the equations of motion and  $n \mathbf{v}$  in the equations of continuity.

The system of equations (1)–(4) allows us to study the interaction of electromagnetic and acoustic waves. We shall be interested in acoustic instabilities in the presence of a strong electromagnetic wave.

### Iteration method

We shall apply the method of iteration with respect to  $\mathbf{E}$  and  $\mathbf{u}$  to study the propagation of an acoustic wave  $\mathbf{u}$  in the presence of an electromagnetic wave  $\mathbf{E}$  and we shall find the attenuation coefficient of sound  $\gamma$  under these conditions in order to understand better the physical nature of the interaction.

The electric field in the system (1) consists of two parts:  $E = E_m + E_u$ , where  $E_m$  is the field of an electromagnetic magnetoplasma wave traveling in the plasma and  $E_u$  appears in the presence of an acoustic wave because of the electrical neutrality conditions of Eq. (3). We shall assume that

$$E_m = {}^{1/2} E_{\omega} e^{-i\omega t}, \quad \mathbf{u} = {}^{1/2} u_0 \exp \{i(qy - \omega_s t)\}, \quad (5)$$

$$E_u = {}^{1/2} E_{u\omega} \exp \{i(qy - \omega_s t)\}, \quad E_{\omega} \parallel x, \quad \mathbf{q} \parallel u_0 \parallel y, \quad \mathbf{H} \parallel z.$$

We shall seek  $v_{e,h}$  and  $n_{e,h}$  in the form of series in powers of  $u$  and  $E_m$ :

$$n = n_{eq} + n^{(1)} + n^{(2)} + n^{(3)}, \quad v = v^{(1)} + v^{(2)} + v^{(3)}.$$

Here,  $n_{eq}$  is the equilibrium electron density;  $n^{(1)}$  and  $v^{(1)}$  are quantities of the first order of smallness;  $n^{(2)}$  and  $v^{(2)}$  are quantities of the second order of smallness, etc. We shall find the attenuation coefficient of sound  $\gamma$  under conditions of electromagnetic pumping by starting from Eqs. (1) and (2) and using Eq. (3) to find an expression for the carrier density, which is proportional to the amplitude of sound and to the square of the electric field of the electromagnetic wave:  $n^{(3)} \propto E_{\omega}^2 u$ . Iterating with respect to  $E_{\omega}$  and  $u$ , we can show that the main contribution to  $n^{(3)}$  comes from the term

$$n^{(3)} = \frac{q}{\omega_s} n_{\omega_s - \omega}^{(2)} v_m, \quad v_m = c \frac{E_m}{H} = \frac{1}{2} v_{\omega} \exp(-i\omega t),$$

where  $n_{\omega_s - \omega}^{(2)}$  is that part of  $n^{(2)}$  which is proportional to  $\exp\{i[qy - (\omega_s - \omega)t]\}$ . It satisfies the equation of continuity

$$\frac{\partial}{\partial t} n_{\omega_s - \omega}^{(2)} + \text{div} (n_{\omega_s}^{(1)} \mathbf{v}_m + n_{eq} v_{\omega_s - \omega}^{(2)} + D \nabla n_{\omega_s - \omega}^{(2)}) = 0, \quad (6)$$

where  $v_{\omega_s - \omega}^{(2)}$  is defined by analogy with  $n_{\omega_s - \omega}^{(2)}$ , whereas  $n_{\omega_s}^{(1)}$  is that part of  $n^{(1)}$  which is proportional to  $u$ . This is due to the fact that in the absence of diffusion, i.e., in the absence of the last term in Eq. (6), we have  $n^{(2)} \rightarrow \infty$  in the limit  $\omega_s \rightarrow \omega$ . The rise of  $n_{\omega_s - \omega}^{(2)}$  and, consequently, the rise of  $n^{(3)}$  are both limited only by the diffusion term:

$$n_{\omega_s - \omega}^{(2)} = \frac{q}{\omega_s - \omega - i\Gamma} (n_{\omega_s}^{(1)} v_m + n_{eq} v_{\omega_s - \omega}^{(2)}), \quad \Gamma = \frac{(qR_e)^2}{3\tau}. \quad (7)$$

Substituting  $n^{(3)}$  into Eq. (4) we find that the attenuation coefficient of sound is given by

$$\gamma_2 = \text{Re} \frac{2Q}{s\rho u_0} n^{(3)} = A \frac{\Gamma \omega_s (\omega_s - \omega)}{(\omega_s - \omega)^2 + \Gamma^2} \left( \frac{v_{\omega}}{s} \right)^2, \quad (8)$$

$$A = \frac{3Q^2}{\epsilon_F (\rho s^2 / n_{eq})}, \quad Q = \frac{Q_e + Q_h}{2}$$

( $\rho$  is the density of the investigated bismuth crystal and  $\varepsilon_F$  is the Fermi energy). The index 2 indicates that the calculated term obeys  $\gamma_2 \propto v_\omega^2 \propto E_\omega^2$ . It follows from Eq. (8) that if  $\omega_s < \omega$ , then the coefficient in question becomes negative  $\gamma_2 < 0$ : amplification of sound becomes possible and an acoustic instability may occur in the presence of pumping. Naturally, this can occur only if  $|\gamma_2|$  is greater than, for example, the pump-independent part  $\gamma_0$  of the electronic attenuation of sound.

The structure of Eq. (8) is similar to the results obtained in Ref. 7 when a quantum-mechanical analysis is made of the  $k \neq 0$  case.

The process of iteration with respect to  $E_m$  and  $u$  makes it possible to identify the mechanism of the interaction of electromagnetic waves traveling in a magnetized electron-hole plasma with acoustic waves in a neutral lattice surrounding the plasma, but it does not work if  $v_\omega \sim s$ , which is true in the experiments on the threshold generation of harmonics in bismuth.<sup>1</sup> However, if the pumping is homogeneous so that  $k = 0$ , the system (1)–(4) can be solved without the requirement of the smallness of  $E_\omega$  and  $v_\omega$ , simply assuming that  $u$  is small.

### Solution for finite values of $E_m$

We shall seek this solution in the form

$$v(y, t) = v_0(y, t) + v_1(y, t),$$

$$n(y, t) = n_{eq} + n_0(y, t) + n_1(y, t).$$

Here,  $(v_0, n_0)$  is the solution of the system for  $Q_e = Q_h = 0$ . Since  $k = 0$ , the functions  $v_0$  and  $n_0$  are proportional to  $E_\omega$  for any value of  $E_\omega$ . However, the corrections  $v_1$  and  $n_1$  are proportional to  $Q \partial^2 u / \partial y^2$ . For convenience, we shall assume that  $E_m = E_\omega \cos \omega t$ . We shall adopt a moving coordinate system:

$$\xi = y - (v_\omega / \omega) \sin(\omega t). \quad (9)$$

In this system Eqs. (1) and (2) for  $v_1$  and  $n_1$  yield the following equations for electrons and holes:

$$m_{e,h} \frac{\partial}{\partial t} \mathbf{v}_1 = \mp e \left( \mathbf{E}_u + \frac{1}{c} [\mathbf{v}_1 \mathbf{H}] \right) \quad (10)$$

$$- Q_{e,h} \nabla^2 \mathbf{u} + \beta_{e,h} \nabla n_1 - \frac{m_{e,h} \mathbf{v}_1}{\tau},$$

$$\frac{\partial}{\partial t} n_1 + n_{eq} \operatorname{div} \mathbf{v}_1 = 0. \quad (11)$$

The term  $n_0 \operatorname{div} \mathbf{v}_1$  is ignored in Eq. (11). An acoustic wave described by Eq. (5) transform in this coordinate system into

$$u_q = (u_0/2) \exp(iq\xi) \exp\{i[-\omega_s t + (qv_\omega/\omega) \sin \omega t]\}. \quad (12)$$

If there is no sound, i.e., if  $u_0 = 0$ , then the carrier is immobile in the new coordinate system. The problem reduces to a calculation of the response to a complex acoustic field of Eq. (12). This problem has been solved, for example, in Ref. 8.

We shall now find the current which appears in the coordinate system (9) in response to a perturbation

$$u_q(\xi, \nu) = \frac{1}{(2\pi)^{1/2}} \int_{-\infty}^{\infty} u_q(\xi, t) e^{i\nu t} dt,$$

and we shall then use Eq. (11) to determine also the Fourier component of the carrier density  $n_1(q, \nu)$  in this system. Returning next to the old coordinate system, we obtain the Fourier component of the carrier density in a coordinate system at rest:

$$n_1(q, \nu) = B \sum_{n, n' = -\infty}^{\infty} \frac{\omega_s - n'\omega}{(\omega_s - n'\omega)^2 + (g/\tau)^2} J_n\left(\frac{qv_\omega}{\omega}\right) J_{n'}\left(\frac{qv_\omega}{\omega}\right) \times \delta[(n' - n)\omega - \omega_s + \nu], \quad (13)$$

$$B = \frac{3}{2} \frac{Q}{\varepsilon_F} (qu_0) \frac{g(1-g)}{\tau} n_{eq},$$

where  $J_n(x)$  is a Bessel function of order  $n$ , and

$$g = 1 - \int_0^{\pi/2} J_0^2(qR \sin \theta) \sin \theta d\theta,$$

$$g = (qR)^2/3 \quad \text{for } qR \ll 1.$$

This derivation is based on Eq. (4.6) from Ref. 8 and on an expansion of  $\exp(iz \sin \omega t)$  in terms of Bessel functions. We shall be interested in the Fourier components  $n_1(q, \nu)$  at the frequency of sound

$$\nu = \pm \omega_s.$$

We shall discuss these cases separately.

1. Substituting  $\nu = \omega$  into the argument of the delta function in Eq. (13), we find that only the terms of the series with  $n' = n$  differ from zero:

$$n_1(q, \omega_s) = B \sum_{n=-\infty}^{\infty} \frac{\omega_s - n\omega}{(\omega_s - n\omega)^2 + (g/\tau)^2} J_n^2\left(\frac{qv_\omega}{\omega}\right). \quad (14)$$

The sum (14) contains resonance terms at frequencies

$$\omega_s \approx n\omega. \quad (15)$$

Since the coefficient of  $\omega_s$  in (15) is unity, the processes described by the series (14) can be called one-phonon. Substituting Eq. (14) into the equation of the motion of the lattice (4), we obtain the attenuation of an acoustic wave (5) for an arbitrary amplitude of an electromagnetic wave:

$$\gamma_{v_\omega}(\omega_s) = A(1-g) \frac{g}{\tau} \omega_s \sum_{n=-\infty}^{\infty} \frac{\omega_s - n\omega}{(\omega_s - n\omega)^2 + (g/\tau)^2} J_n^2\left(\frac{qv_\omega}{\omega}\right). \quad (16)$$

If  $\omega_s \approx \omega$  and  $g \ll \omega\tau$ , Eq. (16) reduces to

$$\gamma_{v_\omega}(\omega_s) = A(1-g) \frac{g}{\tau} \omega_s \left[ \frac{\omega_s - \omega}{(\omega_s - \omega)^2 + (g/\tau)^2} J_1^2\left(\frac{v_\omega}{s}\right) + \frac{2s}{\omega v_\omega} J_0\left(\frac{v_\omega}{s}\right) J_1\left(\frac{v_\omega}{s}\right) \right]. \quad (17)$$

At low electromagnetic wave amplitudes such that  $v_\omega/s \ll 1$

and for  $qR \ll 1$ , the second term in Eq. (17) reduces to the usual expression for the attenuation of sound due to interaction with carriers.<sup>8</sup> The first term then reduces to Eq. (8), which is the additional attenuation proportional to the square of the amplitude of the electric field of the pump wave  $E_{\omega}^2$ .

2. Substituting in the argument of the delta function the relationship  $\nu = -\omega_s$ , we find the condition for the so-called two-phonon parametric decay (dissociation) processes:

$$2\omega_s = p\omega \quad (p = n' - n = 1, 2, 3, \dots), \quad (18)$$

where  $p$  photons decay into two phonons with opposite momenta. If  $p$  is odd, then among the terms of the sum (13) that do not vanish because of the condition (18), there is none which is a resonance term and which becomes infinite in the limit  $g/\tau \rightarrow 0$ . If  $p$  is even, there is such a term:  $n' = n = p/2$ . Therefore, under strong pumping conditions the usual parametric resonance at  $\omega_s = \omega/2$  is relatively weak and the contribution of the process of Eq. (15) at  $\omega_s = \omega$  to the instability increment at the frequency  $\omega_s$  is of the same order as the contribution of the process of Eq. (18) at  $2\omega_s = 2\omega$ . In view of the same dependence on the parameters of the problem, it is difficult to distinguish these two mechanisms experimentally so that we shall use Eqs. (16) and (17) in any subsequent comparison of the theory and experiment.

According to Eq. (16), near each of the multiple frequencies  $n\omega$  ( $n = 1, 2, \dots$ ) there is a narrow frequency interval  $\Delta\omega \approx g/\tau \approx (qR)^2/3\tau$ , where the sum contains one negative term and the absolute value of this term is of the order of  $\tau/(qR)^2$ . Amplification of sound can occur in this frequency interval provided not only that the whole sum is negative, but also that  $\gamma_{v_{\omega}}(\omega_s)$  exceeds the attenuation of sound due to phonons  $\gamma_{ph}(\omega_s)$ . By way of example, we shall consider a frequency interval  $\omega - g/\tau \lesssim \omega_s < \omega$  near the pump frequency  $\omega$ . If  $v_{\omega} \sim s$ ,  $\omega_s \approx \omega \gg 1/\tau$ ,  $qR \ll 1$ , then the first term in Eq. (17) is  $\omega\tau(qR)^{-2}$  times greater than the second because  $\gamma_{v_{\omega}} < 0$ . A comparison of the value of  $\gamma_{v_{\omega}}$  calculated using the known parameters of bismuth with the value of  $\gamma_{ph}$  deduced from the experiments on second sound (Ref. 9),<sup>11</sup> shows that the inequality

$$\alpha = -(\gamma_{v_{\omega}} + \gamma_{ph})$$

is very probably satisfied.

The occurrence of Bessel functions in Eqs. (16) and (17) reflects the circumstance that in the case of instability of amplification of sound we need to transfer energy from an electromagnetic to an acoustic wave. This process occurs most effectively when the amplitude of carrier oscillations under the influence of an electromagnetic wave is of the order of the wavelength of the sound being amplified.

### 3. EXPERIMENTS

We studied experimentally the amplitude and time characteristics of the second harmonic  $2\omega$  generated as a result of interaction of an electromagnetic wave of frequency  $\omega/2\pi = 9.1 \times 10^9$  Hz with bismuth subjected to magnetic fields of  $H \sim 10$ –80 kOe. We used the experimental setup

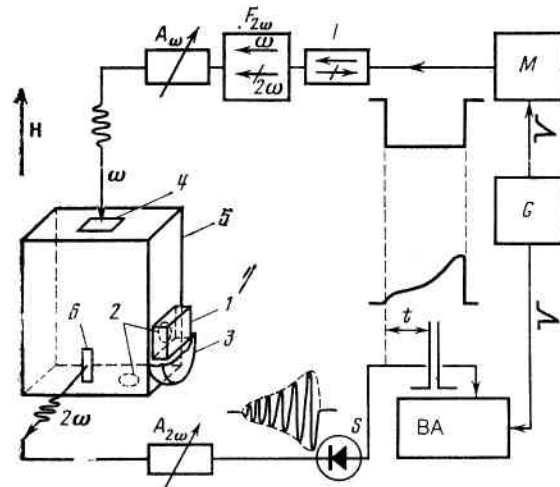


FIG. 1. Schematic diagram of the experimental setup: 1) bismuth sample; 2) apertures; 3) sample holder, acting also as a screen; 4), 6) coupling apertures; 5) resonator;  $A_{\omega}$  and  $A_{2\omega}$  are attenuators tuned to the frequencies  $\omega$  and  $2\omega$ ;  $F_{2\omega}$  is a second harmonic filter;  $I$  is a ferrite isolator;  $M$  is a magnetron;  $G$  is a synchronization pulse generator;  $S$  is a superheterodyne detector; BA is a Boxcar-162 analyzer.

shown in Fig. 1. A magnetron  $M$  generated microwave radiation in the form of rectangular pulses (pulse duration 2–10  $\mu\text{sec}$ , repetition frequency 16 Hz), which reached a rectangular resonator 5 along a waveguide after passing through an aperture 4. A calibrated attenuator  $A_{\omega}$ , an isolator  $I$ , and a system of filters  $F_{2\omega}$  which absorbed the stray second harmonic signal generated by the magnetron itself were placed between the magnetron and the resonator. A sample 1 was pressed against an aperture 2 in the resonator and was therefore part of its wall. The resonator was tuned to the  $TE_{101}$  mode of frequency  $\omega$ , so that only the tangential components of the electric and magnetic fields were experienced by the sample. The radiation of frequency  $2\omega$  was coupled out through an aperture 6, passed through a calibrated attenuator  $A_{2\omega}$ , and was received by a superheterodyne detector  $S$  (intermediate frequency 200 MHz) in a band 10 MHz wide. The detector signal was applied to a Boxcar 162 analyzer and an oscilloscope. The experiments were carried out at temperatures 4.2–12 K in magnetic fields up to 80 kOe.

It is known<sup>10</sup> that magnetoplasma waves with a spectrum  $\omega = \kappa Hk$ , where  $k$  is the wave vector and  $\kappa \sim 10^4$   $\text{cm}\cdot\text{sec}^{-1}\cdot\text{Oe}$ , propagate in bismuth subjected to a strong magnetic field at helium temperatures<sup>10</sup> and the velocity of such waves in a field of  $H = 10^5$  Oe reaches  $V = \omega/k = 10^9$  cm/sec, whereas the direction of propagation is along the normal to the illuminated surface of a sample. Our experiments were carried out in two configurations:  $\mathbf{k} \perp \mathbf{H}$  (using the aperture 2 in the side wall of the resonator—see Fig. 1) and  $\mathbf{k} \parallel \mathbf{H}$  (when the aperture was in the bottom of the resonator); several bismuth single crystals of different shape (disk, plate, rod, parallelepiped) were used and the orientations of the symmetry axes relative to the illuminated surface were varied. We shall report the results for two samples:

1) Bi-1, a plate of  $17 \times 6 \times 0.4$  mm dimensions with the  $C_3$  axis along the normal to the wide face ( $\mathbf{k} \perp \mathbf{H}$  configuration);

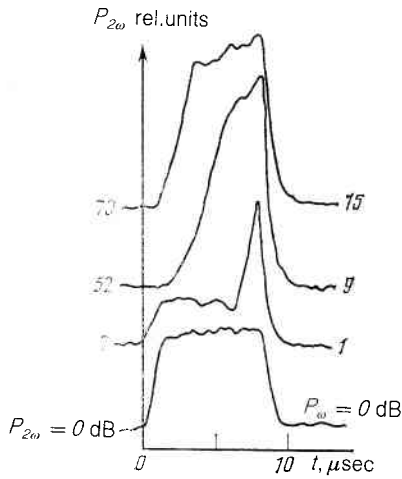


FIG. 2. Profile of the second harmonic pulses generated in sample Bi-2 using different pump powers;  $T = 4.2$  K,  $H = 55$  kOe,  $\mathbf{H} \parallel C_3$ ,  $\mathbf{E}_{\omega} \parallel C_2$ ,  $\mathbf{k} \parallel \mathbf{v}_{\omega} \parallel C_1$ . An increase in the power of the incident wave compared with the power  $P_{\omega}$  for the lower curve is shown on the right and additional attenuation in the receiving channel is shown on the left.

2) Bi-2, a parallelepiped of  $11 \times 9 \times 13$  mm dimensions with the bisector  $C_1$ , binary  $C_2$ , and trigonal  $C_3$  axes oriented at right-angles to the faces to within  $3^\circ$  (both configurations).

The results obtained for other samples were similar.

Figure 2 demonstrates a gradual change in the profile of the  $P_{2\omega}$  pulses on increase in the pump power  $P_{\omega}$ . The lower curve was obtained at a prethreshold incident power of  $P_{\omega} \approx P_{\omega}^{\text{th}}$ . When the threshold was exceeded by a small amount, a rapid growth of the second harmonic power took place at the end of a pulse. A further increase in the pump power shifted the onset of such a growth process toward the beginning of a pump pulse. A comparison of the lower and upper curves in Fig. 2 demonstrated that the increase in the pump power by 15 dB increased the second harmonic power  $P_{2\omega}$  not by three orders of magnitude, as expected in the quadratic regime, but by more than seven orders of magnitude.

A qualitative analysis of the pulse profile, representing the time dependence of the second harmonic power  $P_{2\omega}$ , is given in Fig. 3. The moment  $t = 0$  corresponds to the beginning of the pump pulse. We can see that the increase of  $P_{2\omega}$  with time was initially exponential and this was followed by deviations from the exponential function. A further analysis of the results was made for sample Bi-2 (Fig. 3). Continuing the linear part of the dependence  $P_{2\omega}(t)$  to the point of intersection with the ordinate, we found the initial moment  $P_{2\omega}^{(0)}$  from which the exponential rise of  $P_{2\omega}(t)$  began. When the power  $P_{\omega}$  was altered in a controlled manner by  $\Delta$  dB, then the initial value of  $P_{2\omega}^{(0)}$  changed by  $2\Delta$  dB. This was plotted along the ordinate. Selecting a certain signal level  $W$  in the receiving channel, we could determine the time  $t$  in which the exponentially rising signal reached this value. This gave two points in the exponential part of the dependence  $P_{2\omega}(t)$  for a given pump power  $P_{\omega}$ . Drawing a straight line through these points, we found the slope  $\alpha$  of the straight line representing the growth increment:

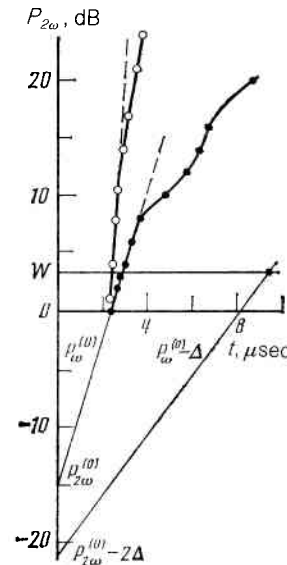


FIG. 3. Time dependences of the power  $P_{2\omega}$  at  $T = 4.2$  K:  $\circ$  Bi-1,  $\mathbf{H} \parallel C_1$ ,  $\mathbf{E}_{\omega} \parallel C_2$ ,  $\mathbf{k} \parallel \mathbf{v}_{\omega} \parallel C_3$ ,  $v_{\omega}/s = 1.0$ ,  $H = 38$  kOe;  $\bullet$  Bi-2,  $\mathbf{H} \parallel \mathbf{k} \parallel C_1$ ,  $\mathbf{E}_{\omega} \parallel C_3$ ,  $v_{\omega} \parallel C_2$ ,  $v_{\omega}/s = 1.3$ ,  $H = 42$  kOe.

$$|\gamma_{v_{\omega}}(\omega)| > \gamma_{ph}(\omega).$$

The functions  $\alpha(v_{\omega})$  determined in this way are plotted in Fig. 4. The most important feature is the existence of a maximum of the function  $\alpha(v_{\omega})$ . The following comments can be made about the position of this maximum. We carried out repeated quite accurate (within about 10%) absolute measurements of  $v_{\omega}$  using a measuring line to find the  $Q$  factor of the resonator and a thermistor bridge to measure the absolute value of the incident power  $P_{\omega}$ . These experiments were carried out on sample Bi-2 in the  $\mathbf{k} \perp \mathbf{H}$  configuration at 4.2 K in a field of about 45 kOe. They gave the values of  $v_{\omega}^{\text{th}}$  given in Table I. However, in the usual experiments made using the stroboscopic integrator the absolute values of  $P_{\omega}$  have been determined with an error as large as 50%. The abscissa in Fig. 4 is subject to the same error. However, the relative values of  $v_{\omega}$  were determined to within 5%.

The method of analysis of the data shown in Fig. 4 can

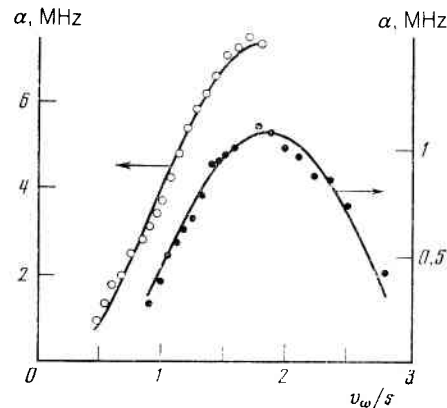


FIG. 4. Dependences of the instability increment on the amplitude of the drift velocity of carriers at  $T = 4.2$  K:  $\circ$  Bi-1,  $\mathbf{H} \parallel C_1$ ,  $\mathbf{E}_{\omega} \parallel C_2$ ,  $\mathbf{k} \parallel \mathbf{v}_{\omega} \parallel C_3$ ,  $H = 38$  kOe;  $\bullet$  Bi-2,  $\mathbf{H} \parallel \mathbf{k} \parallel C_1$ ,  $\mathbf{E}_{\omega} \parallel C_3$ ,  $v_{\omega} \parallel C_2$ ,  $H = 42$  kOe.

TABLE I.

Direction			Threshold drift velocity $v_\omega$ , $10^5$ cm/sec	Maximum velocity of sound in direction of $v_\omega$ (Ref. 17), $10^5$ cm/sec
H	E	$v_\omega$		
$C_1$	$C_2$	$C_3$	$0.73 \pm 10\%$	1.07
$C_1$	$C_3$	$C_2$	$0.92 \pm 10\%$	0.85
$C_3$	$C_2$	$C_1$	$0.96 \pm 10\%$	1.02

also be used to find the dependences of  $\alpha$  on other parameters such as the temperature of a sample for fixed values of  $H$  and  $P_\omega$  (Fig. 5). When the incident power  $P_\omega$  is constant, the change in  $P_{2\omega}$  can be determined simply by measuring the rise time of the second harmonic power  $P_{2\omega}$  to a fixed level.

Extrapolation of the dependence  $\alpha(v_\omega)$  to  $\alpha = 0$  gave the threshold value of the velocity  $v_\omega^{\text{th}}$  and then the threshold power  $P_\omega^{\text{th}}$ . These values corresponded to the onset of an instability after an infinitely long time from the beginning of the incident pulse  $P_\omega$ . It is clear from Fig. 4 that these values were little different from the threshold values of  $v_\omega$  and  $P_\omega$  which could be determined directly after  $10 \mu\text{sec}$  from the beginning of a pulse ( $10 \mu\text{sec}$  was the longest pump duration possible in our experimental system). We ignored this difference and measured  $P_\omega^{\text{th}}$  at the moment of appearance of distortions at the end of the  $P_{2\omega}$  pulse.

Figures 6 and 7 show the dependences of the threshold power  $P_\omega^{\text{th}}$  on the magnetic field and on the temperature of a sample. Calibration values given in Table I made it possible to utilize the  $v_\omega^{\text{th}}/s$  scale in these dependences. This scale stressed the circumstance that the threshold velocity  $v^{\text{th}}$  could be less than or greater than the velocity of sound  $s$ . This was the fundamental difference between the phenomenon under discussion and the mechanism of generation of hypersound in a constant-drift regime.<sup>4</sup>

#### 4. DISCUSSION

We have pointed out in the Introduction that the original experimental observations demonstrated that the instability in the generation of  $P_{2\omega}$  is associated with the amplification of hypersound: an increase in  $P_{2\omega}$  appears at  $v_\omega \sim s$ , the transient processes have characteristic times close to the

times of establishment of a steady state in the constant-drift regime,<sup>4</sup> and the gain in the generation of  $P_{2\omega}$  is close to that observed in Ref. 4. The results of the present paper support strongly this hypothesis.

The exponential growth of  $P_{2\omega}$  with time (Figs. 2 and 3) is an indication of the paramagnetic nature of the process. An indirect confirmation is provided by a strong (exponential) temperature dependence of the value of  $P_{2\omega}$ : an increase in the temperature of a sample by a factor of 3 reduces the second harmonic power  $P_{2\omega}$  by a factor of  $10^3$  for practically the same pump amplitude. It is clear from Fig. 4 that a typical value of the increment at amplitudes twice as high as the threshold is  $\sim 1$  MHz. This means that the characteristic relaxation times of the waves being amplified are  $\sim 1 \mu\text{sec}$ . Such a long relaxation time can only be associated with the phonon system of bismuth, because the time constants of the electron subsystem (such as the momentum relaxation time) are much shorter ( $\tau \approx 10^{-9}$  sec). The existence of the maximum of the instability growth increment at  $v_\omega \approx 2s$  (Fig. 4) makes it necessary to assume that the parametric process is associated with the amplification of hypersound.

The theoretical model in Sec. 2 admits the possibility of two channels of second harmonic generation. The first is identical with that described in the Introduction in a discussion of generation in the constant-drift regime. It postulates amplification of weak sound of frequency  $\omega$  generated on the surface. The second channel can be described as follows. Sound is generated (i.e., it is amplified from the noise level) directly at the frequency  $2\omega$  in the bulk of a crystal and it is then transformed at the surface into an electromagnetic wave of the same frequency. In principle, the theory allows us to distinguish these two channels. We can write down the

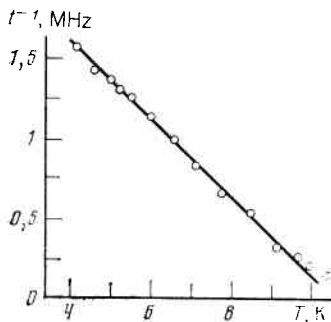


FIG. 5. Temperature dependence of the reciprocal of the growth time of the power  $P_{2\omega}$ : Bi-2,  $\mathbf{H} \parallel \mathbf{k} \parallel C_1$ ,  $\mathbf{E}_\omega \parallel C_3$ ,  $\mathbf{v}_\omega \parallel C_2$ ,  $H = 42$  kOe.

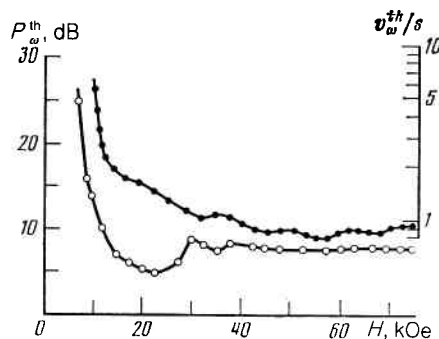


FIG. 6. Dependences of the threshold power  $P_\omega^{\text{th}}$  on the magnetic field  $H$  applied to Bi-2 sample at  $T = 4.2$  K: ●  $\mathbf{H} \parallel C_3$ ,  $\mathbf{E}_\omega \parallel C_2$ ,  $\mathbf{k} \parallel \mathbf{v}_\omega \parallel C_1$ ; ○  $\mathbf{H} \parallel C_1$ ,  $\mathbf{E}_\omega \parallel C_3$ ,  $\mathbf{k} \parallel \mathbf{v}_\omega \parallel C_2$ . The right-hand scale applies only to the upper curve.

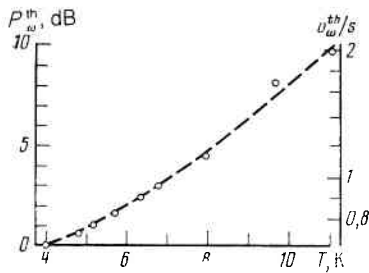


FIG. 7. Temperature dependence of the threshold power  $P_{\omega}^{\text{th}}$ : Bi-2,  $\mathbf{H} \parallel \mathbf{k} \parallel C_1$ ,  $\mathbf{E}_{\omega} \parallel C_3$ ,  $\mathbf{v}_{\omega} \parallel C_2$ ,  $H = 42$  kOe.

formula for the attenuation increment in the form

$$\alpha(v_{\omega}) = \alpha_0 J_n^2(nv_{\omega}/s) - \gamma, \quad n=1, 2, \quad (19)$$

where  $\alpha_0$  and  $\gamma$  are parameters, and  $n = 1$  applies to the first channel and  $n = 2$  to the second. Equation (19) gives different positions of a maximum of the function  $\alpha(v_{\omega})$ :  $v_{\omega}/s = 1.8$  for  $n = 1$  and  $1.5$  for  $n = 2$ . The experimental values are 2.45 for sample Bi-1 and 2.15 for sample Bi-2. Although formally the two theoretical values are within the limits of the 50% error, nevertheless the experiments tend to suggest the first channel. Therefore, we shall carry out a detailed comparison of the experimental results using Eq. (19) and assuming that  $n = 1$ . Variation of the scale along the  $v_{\omega}/s$  axis and of the coefficients  $\alpha_0$  and  $\gamma$  makes it possible to describe very satisfactorily the experimental points (see the continuous curves in Fig. 4). The coefficients  $\alpha_0$  and  $\gamma$  are then quite reasonable:  $\gamma = 0.2$  MHz for Bi-1 and 0.3 MHz for Bi-2 (compare with Ref. 9), whereas  $\alpha_0 = 22$  MHz and 4.3 MHz, respectively. A theoretical estimate gives  $A \approx 3 \times 10^{-4}$  and  $\alpha_0 \approx A\omega \approx 20$  MHz.

We shall now turn to the dependence of the threshold power on  $H$ . We can see from Eq. (17) that the growth increment has a maximum at  $\omega - \omega_s \approx g/\tau \approx (qR)^2/3\tau$ . In the case of bismuth subjected to magnetic fields of 20–80 kOe we find that if  $\omega/2\pi = 10^{10}$  Hz, then  $\omega - \omega_s \sim 2\pi \times 10^6$  Hz, which lies within the  $\sim 10^7$  Hz width of the spectrum of a magnetron pulse. This is important because in the process under discussion it is assumed that there is a “seed” acoustic wave. It also follows from Eq. (17) that at the maximum the term with  $J_1^2$  is practically independent of  $H$ . The value of  $v_{\omega}$

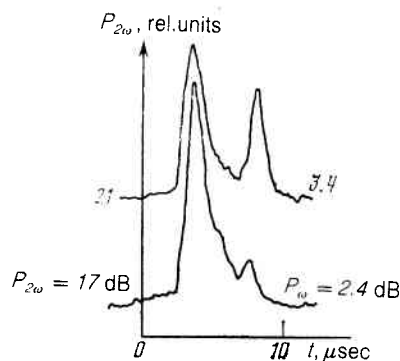


FIG. 8. Profile of the second harmonic pulses obtained at moderate pump powers. The experimental conditions and the notation are the same as for the results obtained in Fig. 2.

is also independent of  $H$ , because the electric field  $E_{\omega}$  of a magnetoplasma wave is proportional to  $H$  (Ref. 10). Consequently, in strong magnetic fields the threshold power  $P_{\omega}^{\text{th}}$  is independent of  $H$ , as found experimentally (Fig. 6). A reduction in the magnetic field intensity may bring into operation various factors so that the maximum of  $\alpha$  begins to edge out of the magnetron band. It is possible that an increase in the pump power is due to the fact that the pumping inhomogeneity begins to play a role. The nonmonotonic dependence  $P_{\omega}^{\text{th}}(H)$  observed in moderate fields is due to oscillations of the density of states at the Fermi level.<sup>1</sup> Such oscillations of nonlinear threshold characteristics of bismuth have been observed earlier.<sup>11</sup>

We shall now discuss the dependence of the threshold on the temperature of a sample. According to Eq. (17), the coefficient  $\alpha_0$  in Eq. (19) is independent of  $\tau$ . Therefore, the observed dependence of the increment  $\alpha(v_{\omega})$  on  $T$  in Eq. (19) should be contained in  $\gamma$  and we know that  $\gamma$  is related to the scattering of sound on phonons. There are several mechanisms for the attenuation of sound by phonons.<sup>12</sup> Figure 5 shows the temperature dependence of a quantity proportional to the growth increment. This dependence is nearly linear, so that in the case of Bi at frequencies  $\omega/2\pi \approx 10^{10}$  Hz the decay mechanism of the relaxation of sound by phonons predominates, which is not surprising at very high frequencies.<sup>12</sup>

We shall now consider the problem of the subsequent evolution of a parametric instability and the resultant harmonic generation processes. This topic is currently the subject of intensive theoretical studies and also of model experiments because of the appearance of soliton-like generation regimes and also of stochastic (turbulent) regimes in systems with a small number of interacting waves.<sup>13,14</sup> If we modify the experimental conditions somewhat, for example by altering the value of  $H$  and  $P_{\omega}$ , we can change greatly the profile of a  $P_{2\omega}$  pulse and obtain not the pulses in Fig. 2 but a different result (see Fig. 8, which shows pulses obtained at intermediate values of  $P_{\omega}$  relative to those recorded at 1 dB and 9 dB in Fig. 2). We even reported earlier<sup>1</sup> cases when in a period of 10  $\mu\text{sec}$  there were three generation peaks. This generation regime is clearly associated with a modulation instability of a growing acoustic wave of frequency  $\omega$ . The same model of modulation instability predicts also a stochastic regime of the generation of sound.<sup>14</sup> We cannot exclude the possibility that this process is responsible for the appearance of radioelectric current noise in bismuth when a sample is subjected to a strong microwave radiation.<sup>3,15</sup>

## 5. CONCLUSIONS

We can regard it as established that the threshold generation of the second harmonic of microwave radiation in Bi subjected to strong magnetic fields is associated with parametric amplification of hypersound at a frequency located in a narrow spectral interval close to the pump frequency. In contrast to an acoustoelectronic instability associated with the Vavilov-Cherenkov effect,<sup>2,16</sup> in our case the instability increment is positive in a narrow frequency interval which

can be varied by altering the frequency of the incident radiation.

The authors are grateful to I. A. Voropanova for growing the samples and to V. V. Shvyrkin for technical help.

<sup>1</sup>The value  $\gamma_{\text{ph}} \approx 10^7$  sec was obtained in Ref. 9 for thermal phonons with  $T \approx 4$  K; in our case the phonon energy was about 0.3 K and, consequently, the relaxation frequency was at least an order of magnitude less:  $\gamma_{\text{ph}}(\omega) \approx 10^6$  sec.

<sup>1</sup>S. A. Vitkalov, V. F. Gantmakher, and G. I. Leviev, *Pis'ma Zh. Eksp. Teor. Fiz.* **39**, 540 (1984) [*JETP Lett.* **39**, 660 (1984)].

<sup>2</sup>L. Esaki, *Phys. Rev. Lett.* **8**, 4 (1962).

<sup>3</sup>G. I. Leviev and É. G. Yashchin, *Pis'ma Zh. Eksp. Teor. Fiz.* **18**, 298 (1973) [*JETP Lett.* **18**, 174 (1973)].

<sup>4</sup>S. A. Vitkalov, V. F. Gantmakher, and G. I. Leviev, *Solid State Commun.* **54**, 1091 (1985).

<sup>5</sup>É. G. Yashchin, *Fiz. Tverd. Tela (Leningrad)* **22**, 2293 (1980) [*Sov. Phys. Solid State* **22**, 1335 (1980)].

<sup>6</sup>T. Yamada, *J. Phys. Soc. Jpn.* **20**, 1647 (1965).

<sup>7</sup>A. P. Kopasov and V. Ya. Demikhovskii, *Fiz. Tverd. Tela (Leningrad)* **15**, 3589 (1973) [*Sov. Phys. Solid State* **15**, 2395 (1974)].

<sup>8</sup>M. H. Cohen, M. J. Harrison, and W. A. Harrison, *Phys. Rev.* **117**, 937 (1960).

<sup>9</sup>V. Narayanamurti and R. C. Dynes, *Phys. Rev. Lett.* **28**, 1461 (1972).

<sup>10</sup>V. S. Édel'man, *Usp. Fiz. Nauk* **123**, 257 (1977) [*Sov. Phys. Usp.* **20**, 819 (1977)].

<sup>11</sup>É. G. Yashchin, *Fiz. Tverd. Tela (Leningrad)* **22**, 1740 (1980) [*Sov. Phys. Solid State* **22**, 1014 (1980)].

<sup>12</sup>V. L. Gurevich, *Kinetika fononnykh sistem (Kinetics of Phonon Systems)*, Nauka, M., 1980.

<sup>13</sup>Y. Kuramoto and T. Yamada, *Prog. Theor. Phys.* **56**, 679 (1976).

<sup>14</sup>M. I. Rabinovich and A. L. Fabrikant, *Zh. Eksp. Teor. Fiz.* **77**, 617 (1979) [*Sov. Phys. JETP* **50**, 311 (1979)].

<sup>15</sup>É. G. Yashchin, *Fiz. Tverd. Tela (Leningrad)* **19**, 1188 (1977) [*Sov. Phys. Solid State* **19**, 693 (1977)].

<sup>16</sup>A. R. Hutson, J. H. McFee, and D. L. White, *Phys. Rev. Lett.* **7**, 237 (1961).

<sup>17</sup>Y. Eckstein, A. W. Lawson, and D. Reneker, *J. Appl. Phys.* **31**, 1534 (1960).

Translated by A. Tybulewicz